JACS
JOURNAL OF THE AMERICAN CHEMICAL SOCIETY
pubs.acs.org/JACS
Article

Calix[4]trap: A Bioinspired Host Equipped with Dual Selection Mechanisms

Zhenchuang Xu, Nie Fang, and Yanchuan Zhao*

Cite This: J. Am. Chem. Soc. 2021, 143, 3162–3168
Read Online

ABSTRACT: Regulation of recognition events evolving in time and space is vital for living organisms. During evolution, organisms have developed distinct and orthogonal mechanisms to achieve selective recognition, avoiding mutual interference. Although the merging of multiple selection mechanisms into a single artificial host may lead to a more adaptable recognition system with unparalleled selectivity, successful implementation of this strategy is rare. Inspired by the intriguing structures and recognition properties of two well-known biological ion binders—valinomycin and K^+ channels—we herein report a series of hosts equipped with dual guest selection mechanisms. These hosts simultaneously possess a preorganized binding cavity and a confined ion translocation tunnel, which are crucial to the record-setting K^+/Na^+ selectivity and versatile capabilities to discriminate against a wide range of ion pairs, such as K^+/Rb^+, K^+/Ba^{2+}, and Rb^+/Cs^+. Mechanistic studies verify that the host's portal is capable of discriminating cations by their size, enabling varied ion uptake rates. The confined tunnel bearing consecutive binding sites promotes complete desolvation of ions during their inclusion into the buried cavity, mimicking the ion translocation within ion channels. Our results demonstrate that the capability to manipulate guest recognition both in equilibrium and out-of-equilibrium states allows the host to effectively discriminate diverse guests via distinct mechanisms. The strategy to merge orthogonal selection mechanisms paves a new avenue to creating more robust hosts that may function in complex biological environments where many recognition events occur concurrently.

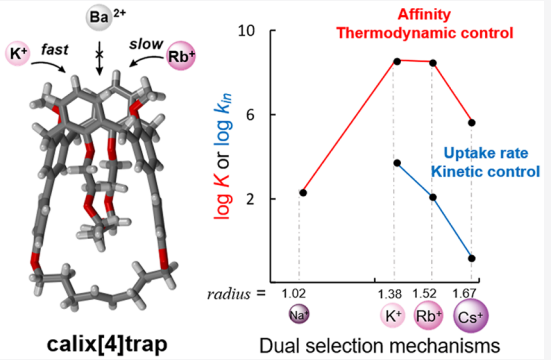

INTRODUCTION

Molecular recognitions ubiquitously occur in life activities. Metal ions are vital to various physiological processes, ranging from heartbeat and muscle contraction to signal transduction.[1−3] Through evolution, living organisms have mastered the skill of selective binding and transporting ions by creating task-oriented functional units.[4,5] Prominent examples include valinomycin and K^+ channels, both of which allow for ion trafficking across the cell membrane.[6] Valinomycin possesses a rigid scaffold and utilizes six carbonyl oxygens to form an ion binding cavity (Figure 1A).[7] The preorganized structure along with the optimal cavity size account for its much stronger affinity to K^+ than Na^+. In contrast, kinetic factors dominate in the selection mechanism of K^+ channels, in which ions are conducted at vastly different rates. The successive binding sites within the channel's selectivity filter constitute an ion transporting highway, where strict permeation of K^+ is not only dictated by the ion's charge and radius but also by the ease for the ion to undergo desolvation (Figure 1A).[8−11] These two examples demonstrate cases in which nature achieves guest discrimination through manipulating either binding affinities or rates. Although bionic designs are mostly directed to mimic one specific biological structure and function,[12−21] we asked what if we combine the selection strategies of valinomycin and K^+ channels and realize them in a single host? Could this act as new design wisdom to achieve more versatile and record-setting discrimination ability? Here, we implement this idea in developing a new class of biomimetic hosts that we name calix[4]traps because of their structural similarity to pitcher plant (Figure 1B). Calix[4]traps possess record-breaking K^+/Na^+ selectivity superior to valinomycin and other artificial ion hosts, whereas their confined binding tunnel structurally mimics K^+ channels, enabling varied ion uptakes rates. The embedding of orthogonal selection strategies renders calix[4]traps capability to effectively separate a variety of ion pairs, such as Na^+/K^+, K^+/Rb^+, K^+/Ba^+, and Rb^+/Cs^+ via distinct mechanisms. The unique structure of calix[4]trap allows the characterization of ion translocation from the tunnel's portal to the internal binding cavity, serving as an ideal model to understand successive recognitions in a confined environment.

Received: November 23, 2020
Published: February 19, 2021

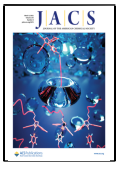

https://dx.doi.org/10.1021/jacs.0c12223
J. Am. Chem. Soc. 2021, 143, 3162−3168

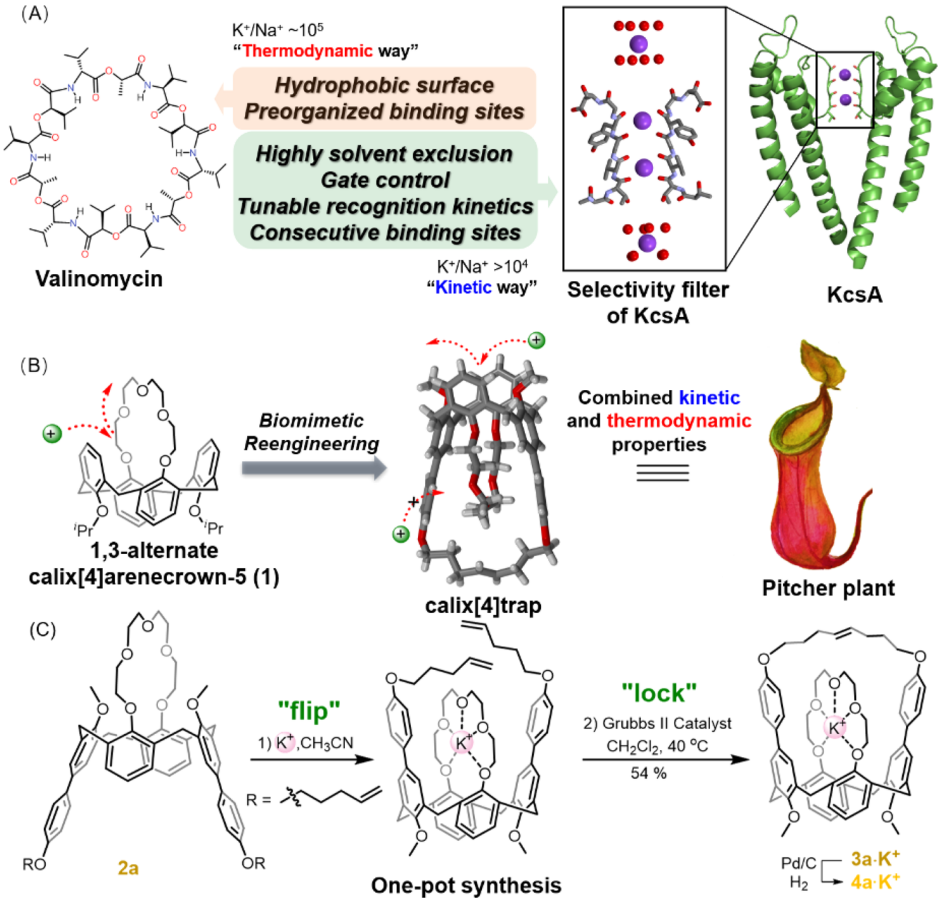

Figure 1. Design and synthesis of calix[4]traps. (A) Valinomycin and the selectivity filter of K^+ channel of streptomyces A (KcsA) (Protein Data Bank, 1K4C). (B) Image of a pitcher plant, the structure of 1,3-alternate calix[4]crown-5 (**1**), and X-ray single-crystal structure of calix[4]trap **3a**. The picture of the pitcher plant was crafted by Ms. Suzhen Zhu. (C) The "flip" and "lock" strategy used to synthesize the designed ion hosts. Hydrogenation of double bond of **3a**·K^+ affords **4a**·K^+.

Inspired by the unique structure and properties of valinomycin and K^+ channels, we sought to create a biomimetic ion host that discriminates ions through both thermodynamic and kinetic selection mechanisms. Given the fact many ion hosts display excellent thermodynamic ion selectivity,[22,23] our effort is directed to confer established ion hosts with a tunnel-like ion transport path that is essential for kinetically varied ion binding. We see the 1,3-alternate calix[4]arenecrown-5 (**1**) as a great candidate on which to perform the structural reengineering because it functionally resembles valinomycin and displays recording-setting K^+/Na^+ selectivity.[24,25] Unlike the orderly ion transport occurring within ion channels, metal ions approach **1**'s central cavity from diverse directions, resulting in rapid and poorly controlled binding processes. Despite the exceptional K^+/Na^+ selectivity, **1** fails to effectively discriminate K^+ from metal ions of comparable sizes, such as Rb^+ and Ba^{2+}. We thus wonder whether the not-yet-owned discrimination ability could be conferred by a confined binding tunnel biomimetic to K^+ channel, where ions are uptaken with distinct rates. To test the feasibility of this idea, we first attempted to encapsulate **1**'s ligating etheric oxygens within a confined tunnel to block the original ion binding path. We envision that the extension of the arene clefts on the calixarene's lower rim would fully cover the crown-5 motif from left and right, thereby preventing ions from squeezing in from both sides (Figure 1B). Under this circumstance, the calix[4]arene cavitand would become the only portal for ion uptake. We are also aware that a proper linkage between the aromatic clefts is needed to restrain the conformational flexibility to prevent the opening of clefts. In the re-engineered host **3a**, the two methoxy groups on the tunnel mouth along with the etheric oxygens of crown-5 constitute spatially consecutive binding sites that elongate into the confined internal space (Figure 1B, C). These structural features resemble those of K^+ channels and would enable successive recognitions during the inclusion of the ion into the buried cavity. Through this strategic modification, we were able to impart a host with the capability to kinetically discriminate ions with minimal alteration of its original ion binding environment.

RESULTS AND DISCUSSION

A "flip and lock" strategy was utilized to prepare the target host **3a** with binding sites wrapped around by molecular clefts (Figure 1C). The synthetic route design is inspired by a classical conformational switch observed in calixarene-based crown ethers upon K^+ binding (Figure 1C), which is likely driven by the favorable cation-π interactions proposed by Prodi, Casnati, and co-workers.[26] As depicted in Figure 1C, compound **2a** was first mixed with K^+ in acetonitrile to switch to 1,3-alternate structure (Figure S5). Acetonitrile was then replaced by dichloromethane to perform the subsequent ring-closing metathesis (RCM),[27] affording **3**·K^+ in fixed conformation (Figure 1C). To gain more insights on the

https://dx.doi.org/10.1021/jacs.0c12223
J. Am. Chem. Soc. 2021, 143, 3162−3168

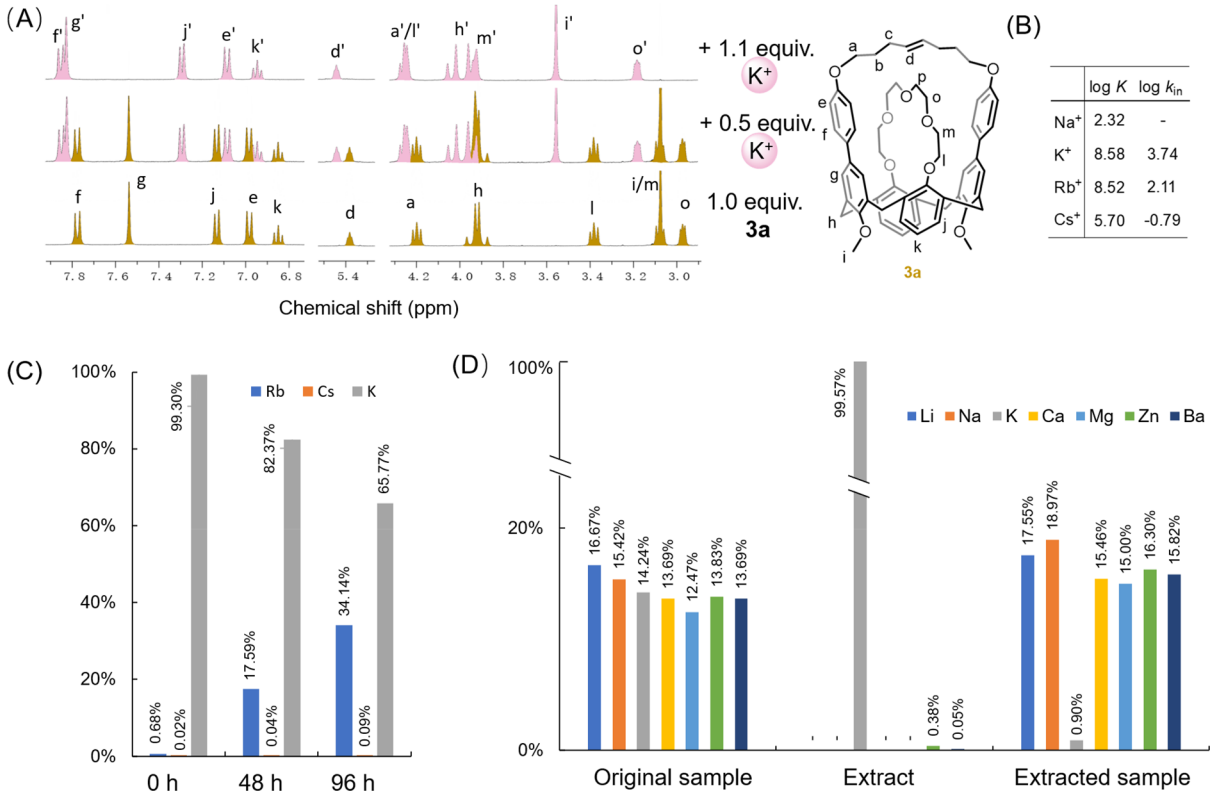

	log K	log k_{in}
Na^+	2.32	-
K^+	8.58	3.74
Rb^+	8.52	2.11
Cs^+	5.70	-0.79

Figure 2. Ion recognition behaviors and ions separation experiments. (A) ^{1}H NMR titration of calix[4]trap **3a** with K^+ in d_6-acetone. Two sets of NMR signals corresponding to **3a** and **3a**·K^+ were observed, suggesting that the exchange between free and bound K^+ is slow on the NMR time scale. (B) Measured log K (binding affinity, in d_6-acetone/$CDCl_3$ = 4:1 (v/v)) and log k_{in} (associating rate constant, in d_6-acetone/$CDCl_3$ or acetone/$CHCl_3$ = 4:1 (v/v)) of **3a** at 25 °C. (C) Separation of K^+, Rb^+, and Cs^+ based on the distinct complexation rates. Ion compositions were measured at different times using ICP-MS. (D) Selective cation extraction using **3a** in the presence of various cations. Hyphens indicate that the concentration of the measured cation was lower than the limit of detection.

conformational flipping and cation−π interaction in our system, we performed ^{1}H NMR analysis of the binding between **2a** and K^+. As shown in Figure S5, upon the addition of K^+ to a solution of **2a**, **2a** underwent a conformational switch from the cone configuration to mainly the 1,3-alternate conformer. A pronounced downfield shift of the resonance of H_f was observed, which supports the presence of the cation−π interaction. The internal olefin was mostly formed in the *E*-configuration during RCM, probably due to the lower ring strain during cyclization (Figure 1C). We also attempted to use shorter alkenyl chains for the RCM, whereas only oligomeric substances were produced. As the bound K^+ is deeply buried, the obtained **3a**·K^+ displays considerable stability, preserving the trapped K^+ during chromatographic purification. In contrast, the K^+ of **2a**·K^+ is readily removed during the workup, supporting the significant contribution of shielding on stability.[28,29] As expected, a significant increase in K^+ affinity was observed for all the calix[4]traps compared to that of conformationally unflipped host **2a** (Table S9). The metal-free host **3a** was then accessed by using cryptand[2.2.2] as the K^+ scavenger in refluxing acetonitrile wherein **3a** precipitates out, allowing for facile isolation. The X-ray single-crystal structure of **3a** verified a structure with consecutive and deeply buried ligating sites. These structural features resemble those of the selective filter of KcsA, where multiple carbonyl ligating groups within the channel constitute an ion transporting highway.

Following the encouraging initial results, we next examined whether our design strategy retains the exceptional K^+/Na^+ selectivity of host **1**. It is noteworthy that the nature of anion has a pronounced influence on the recognition of metal ions because the binding is accompanied by the change in both ion solvation state and electrostatic interactions between ion pairs.[22] To minimize the influence of anion and ensure a high solubility of the metal salts under our experimental conditions, we used the weakly coordinating $C_4F_9SO_3^-$ as the counterion for all the measurements. Competitive experiments with **1** revealed that **3a** is 1.46 times stronger at binding with K^+ and 3.16 times weaker at binding to Na^+; the K^+/Na^+ selectivity increases by 4.61 times after the structural reengineering (Figures S12−14). A more rigidified binding environment could account for the high affinity of **3a** toward K^+, whereas the attenuated affinity to Na^+ is unexpected because an increase in preorganization was envisioned to strengthen binding to both K^+ and Na^+. We assume that the isolated binding cavity of **3a** minimizes the energetically favored interactions between the bound ion and species in the solvent, which thereby leading to fewer ligating sites and inferior affinity after binding (Figures S15 and 16). This assumption is also supported by the observation that **3a** fails to bind Na^+ in the presence of an excess amount of water, whereas the affinity of **1** to Na^+ only drops by about 2 times under the same conditions (Figure S16). In analogy to K^+ channels, calix[4]-trap **3a** is capable of harnessing distinct ion solvation properties and confined space to achieve better ion discrimination. Our findings thus indicate that the modulation of solvent accessibility to the binding pockets might be a viable way to further boost the record-setting selectivity (for a list of K^+/Na^+ selectivities of other ion hosts, see Table S10).

https://dx.doi.org/10.1021/jacs.0c12223
J. Am. Chem. Soc. 2021, 143, 3162−3168

Considering that the K^+/Na^+ selectivity in aqueous solution is more relevant to biological applications, we attempted to embed calix[4]trap **3a** in liposomes following previously reported methods. However, it was found that calix[4]trap **3a** existed in the solid form under these conditions and was not mixable with liposomes in water. This behavior is likely due to the low solubility of **3a** in both water and liposomes, which is reasonable given the fact that **3a** possesses a highly rigid skeleton rich in aromatic rings. To test the K^+/Na^+ selectivity of calix[4]traps in an aqueous solution, where the K^+ and Na^+ ions are highly hydrated, we performed a structural modification on **3a** by replacing the methoxy group on the tunnel mouth with a polyethylene glycol (PEG) chain. The structurally modified calix[4]trap **3a-PEG**, albeit not soluble in pure water, possesses good solubility in d_6-acetone/D_2O (v/v = 1/1), which allows the measurement of binding selectivity toward hydrated K^+ and Na^+. The investigation showed that the K^+/Na^+ selectivity of **3a-PEG** in this solvent mixture is higher than $1 \times 10^{5.8}$, indicating that excellent K^+/Na^+ selectivity is retained in the presence of water (page S39 in the Supporting Information). The high K^+/Na^+ selectivity is also supported by the mass spectroscopy experiments (Figure S23), in which the mass signal related to [**3a-PEG**+Na]$^+$ was not observed even if the concentration of Na^+ is 50 times higher than that of K^+.

To further explore whether the biomimetic binding tunnel confers calix[4]trap **3a** new discrimination ability, we investigated the binding properties of **3a** to metal ions of comparable size. Discrete sets of NMR signals were observed for **3a** and **3a**·M (M = K^+, Rb^+), suggesting the ion recognition is slow on the NMR time scale (Figure 2A). Interestingly, although the binding strength of **3a** to K^+ and Rb^+ are quite similar (Figure 2B), the rate constants for associations (log k_{in}) differ significantly, being 3.74, and 2.11 for K^+, and Rb^+, respectively (Figure 2B). These values reflect quite sluggish associations, which are usually not observed with crown ethers and cryptands. In an experiment to test the competitive binding of K^+, and Rb^+ to **3a**, a solution of **3a** was added to a cool acetone solution containing K^+ (2.0 equiv) and Rb^+ (2.0 equiv) at −78 °C. When the NMR analysis was performed immediately after the mixture was warmed to rt, **3a**·K^+ was formed exclusively (Figure S17). Over time at room temperature, the replacement of bound K^+ by Rb^+ occurs but at a very low rate. In line with our initial design, **3a** behaves like a biomimetic selective filter, enabling size-dependent ion uptake. Notably, the kinetically differed ion recognition allows **3a** to effectively discriminate K^+ from Rb^+, a property that is not possessed by the original host **1**. Given the fact that optimal K^+/Na^+ selectivity is usually accompanied by an inferior K^+/Rb^+ selectivity (e.g., $K^+/Rb^+ \sim 1$ for KcsA),[8] our strategy provides a unique solution to address this dilemma. As a step to further examining the selectivity of **3a** toward different ions, ^{1}H NMR spectra were recorded for mixtures of **3a** and a series of alkaline-earth metal ions, including Mg^{2+}, Ca^{2+}, Sr^{2+}, and Ba^{2+}. Surprisingly, none of these ions show appreciable binding affinities to **3a** (Figure S7), which is in sharp contrast to the chelating properties of crown ethers and cryptands.[30,31] The negligible affinity of **3a** to alkaline-earth metal ions can be ascribed to its confined tunnel-like structure, wherein the metal ions have to be stripped off their counterions to be swallowed into the buried cavity, an energetically unfavorable process, especially for divalent metal ions.[32] In line with this assumption, the receptor **2a**, the precursor of **3a** without ring closure, shows substantial affinities to Ba^{2+} besides alkali metal ions (Figure S8).

We next examined whether varied ion uptake rates and negligible affinity to alkaline-earth metal ions could confer **3a** unique separation properties. The separation system was designed to take the advantage of the distinct solubility and high kinetic stabilities of ion-complexed **3a** and metal salts. In one experiment, **3a** was mixed with an acetone solution containing K^+, Rb^+, and Cs^+ at low temperature and then warmed to rt for ion complexation. The addition of dichloromethane leads to the precipitation of unchelated metal salts, which were readily separated from ion-complexed **3a** through filtration. We found the extraction selectivity is dependent on the operation time, with the highest selectivity (K:Rb > 99:1) observed when the precipitation was conducted immediately after mixing. As the operation was prolonged to allow ion exchange to occur, inferior extraction selectivity has resulted. When the mixture was placed at rt for 96 h, the ratio between **3a**·K^+ to **3a**·Rb^+ became 1.5:1(Figure 2C), verifying a kinetically controlled ion uptake. By using a similar procedure but without resorting to low operation temperatures, the selective extraction of K^+ from a mixture of Li^+, Na^+, K^+, Mg^{2+}, Ca^{2+}, Zn^{2+}, and Ba^{2+} was achieved. These separation properties support that **3a** could effectively discriminate ions through both thermodynamic and kinetic selection mechanisms. Compared to hosts displaying exclusive ion binding property, the discrimination ability of **3a** is more versatile, allowing effective ion extraction from a broad range of ion pairs, such as Rb^+/Cs^+ (Figure S19), Rb^+/Ba^{2+}, and Cs^+/Ba^{2+} (Figure 2C). The unique structural features of **3a** enable multiple selection mechanisms operating orthogonally, potentially providing unparalleled adaptability when functioning in a complex biological environment.

Given the fact that conformational fluctuation of K^+ channels has profound influences on the ion conduction,[33,34] we turned our attention to modify the arene clefts and the linker to tune the kinetics of ion uptake. Calix[4]traps **3b** and **4c** were prepared using a similar procedure depicted in Figure 1C. For calix[4]trap **4c**, hydrogenation was performed because a mixture of *E* and *Z* stereoisomers were afforded during the RCM (Figure 3A). Although the introduced substituents are distal to the tunnel mouth, their influences on the affinity and the ion association rates are significant (Figure 3B, C). Compared with **3a**, etheric oxygens of **3b** and **4c** adopt arrangements unfavorable for ligating metal ions, which may result in higher organizational demands and lower affinity (Figure S42). The different ion uptake rates could be attributed to substitution-induced conformational adjustment, which alters the confined internal environments and portals of calix[4]traps. As depicted in Figure S41, the incorporation of substituents has a significant influence on the distance between the aromatic sidewalls around the crown-ether moiety. As the distance between the sidewall becomes longer, a drop in the affinity to K^+ was observed, probably due to the weakened $K^+-\pi$ interaction. To test whether the distinct flexibility of the alkyl and alkenyl linkage has a pronounced influence on the ion binding, we prepared calix[4]trap **4a** via hydrogenation of **3a**. The investigation showed that the recognition properties of calix[4]trap **4a** toward K^+, Rb^+, and Cs^+ are similar to those of **3a** (Figure 4B and Table S15), which indicates that the hydrogenation of the alkenyl linkage only has a minimal influence on the ion recognition properties of calix[4]traps. Unlike most ion hosts that bind ion rapidly by a diffusion-

https://dx.doi.org/10.1021/jacs.0c12223
J. Am. Chem. Soc. 2021, 143, 3162−3168

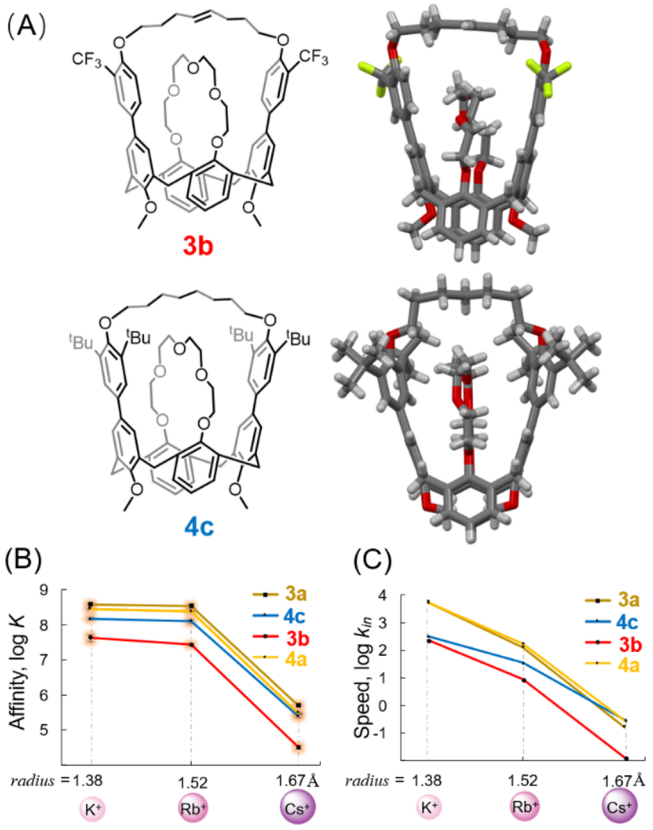

Figure 3. Kinetic and thermodynamic data for the association between K^+, Rb^+, and Cs^+ and various ion hosts. (A) Chemical and X-ray single-crystal structures of calix[4]traps **3b** and **4c**. (B) Measured log*K* for complexation of various metal cations with calix[4]traps **3a**, **3b**, **4a**, and **4c** in d_6-acetone/$CDCl_3$ = 4:1 (*v*/*v*) at 25 °C. (C) Measured log k_{in} for complexation of various metal cations with calix[4]traps **3a**, **3b**, **4a**, and **4c** in d_6-acetone/$CDCl_3$ = 4:1 (*v*/*v*) at 25 °C.

controlled kinetics,[12,13] calix[4]traps showed a linear relationship between ion radius and association rate, with the slowest ion capture observed in the formation of **3b**·Cs^+. Besides, all ion-complexed calix[4]traps display considerable kinetic stability and retarded ion release. The observed half-lives for dissociation of K^+ and Rb^+ from the calix[4]traps span over a range from hours to several days (Table S2). Collectively, the confined tunnel-like structure result in retarded ion uptake and release, allowing the recognition kinetics to be finely tuned.

The tunnel mouth of biological ion channels plays a crucial role in the initial ion desolvation, which promotes selective ion transport. However, the ion translocation within a confined molecular tunnel was rarely experimentally characterized. Because of the slow uptake of Cs^+ with calix[4]trap **3b**, we were fortunate to observe shifts of **3b**'s NMR resonances before the inclusion of Cs^+ into the buried cavity. Upon the addition of varying amounts of Cs^+, the chemical shift of the resonance H_f changes gradually (Figure 4B), indicating that the first step of Cs^+ uptake is fast on the NMR time scale. Pronounced NMR shifts were observed in the methoxy groups along with the nearby aromatic protons, whereas the ^1H signals of the buried crown-5 are minimally perturbed (Figure 4A). These observations can be rationalized by an association within the tunnel mouth (Figure 4B). As evidenced by the shift of ^1H signals of methylene bridges, subtle conformational change was induced upon ion recognition. Over time, NMR shows that Cs^+ slowly squeezes in the tunnel and enters into the buried cavity. Base on the ^1H NMR titration experiments, the affinity of **3b**'s tunnel mouth with Cs^+ was determined to be 126.5. Furthermore, the uptake rate and association constant for the second step of the ion uptake were calculated to be $1 \times 10^{-3.68}$ s^{-1} and $1 \times 10^{2.41}$, respectively (for details, see page S44 in the Supporting Information). We found that the uptake of Cs^+ into the deep cavity of **3b** is quite slow. When the concentration of **3b** (2.9 mM) was mixed with $CsSO_3C_4F_9$ (2.3 equiv), 83 and 97% of **3b** was converted into **3b**·Cs^+ after 7.3 and 45 h, respectively. Notably, the ion uptake rate is found to be dependent on the anion. When $CF_3CO_2^-$ is used as the

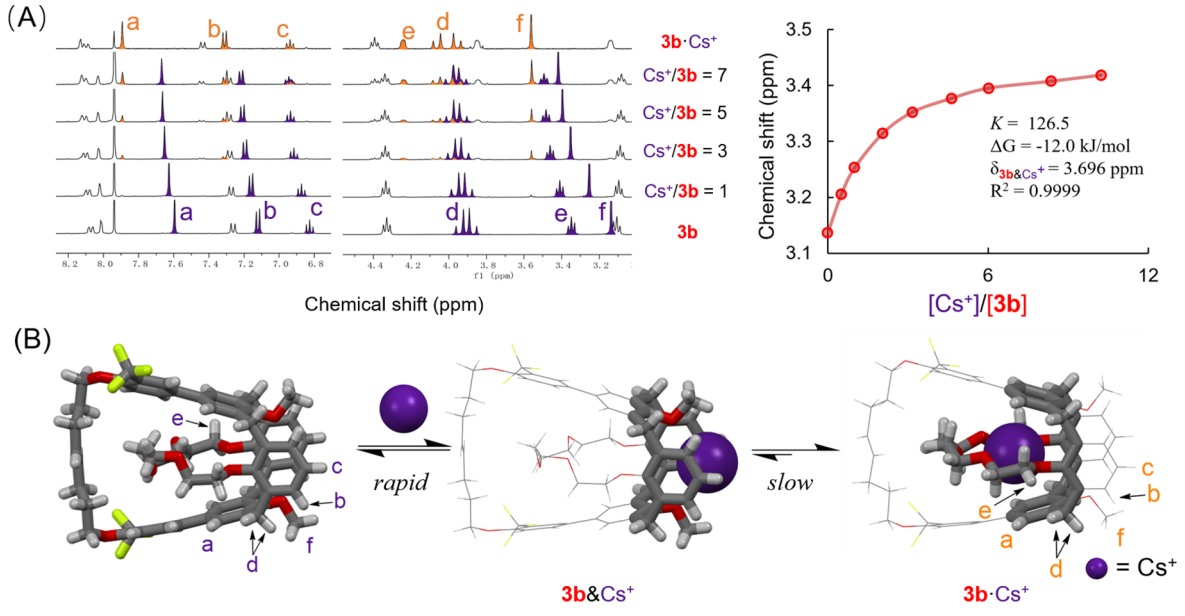

Figure 4. Investigation of the ion recognition pathway. (A) ^1H NMR titration of calix[4]trap **3b** with Cs^+ before the inclusion of Cs^+ into the buried cavity. (B) Proposed ion recognition path for the uptake of Cs^+ with calix[4]trap **3b**. For detailed assignments, see Figures S26.

https://dx.doi.org/10.1021/jacs.0c12223
J. Am. Chem. Soc. 2021, 143, 3162−3168

counterion instead of $C_4F_9SO_3^-$, the rate for Cs^+ to get into the deep cavity becomes slightly slower (Figure S25), probably because of the better coordinating property of $CF_3CO_2^-$. The same binding pathway is also adapted by Rb^+ and K^+, as deduced by NMR experiments at lower temperatures (Figures S28 and 29). Therefore, the tunnel mouth serves as a gatekeeper in this sequential dual recognition system, which senses the ion before uptake (Figure 4B). This interesting behavior is reminiscent of the gated ion transport in biosystems.[35]

CONCLUSION

By mimicking the preorganized binding sites of valinomycin and the consecutive ligating sites of K^+ channels, we synthesized a series of novel ion hosts, which simultaneously possess a deeply buried binding cavity and a confined ion translocation tunnel. Mechanistic studies verify that the host's portal could discriminate metal cations by their size, enabling varied ion uptake rates. The confined tunnel bearing consecutive binding sites promotes complete desolvation of ions during their inclusion into the buried cavity, mimicking the ion translocation within biological ion channels. The merging of selection strategies learned from valinomycin and K^+ channels proved useful to further boost the record-setting selectivity and make possible the modulation of successive recognition events evolving in space and time. The capability to manipulate guest recognition both in equilibrium and out-of-equilibrium states allows the host to effectively discriminate diverse guests via distinct mechanisms. The strategy to merge orthogonal selection mechanisms into a single host offers new opportunities to create more robust supramolecules and functional materials that may function in complex biological environments.

ASSOCIATED CONTENT

Supporting Information

The Supporting Information is available free of charge at https://pubs.acs.org/doi/10.1021/jacs.0c12223.

Experimental procedures, characterization details, experiments to investigate binding constants and kinetics, and copies of ^1H, ^{19}F, and ^{13}C NMR spectra for new compounds (PDF)

Accession Codes

CCDC 2026510−2026513, 2026515−2026516, 2026521−2026522, 2027069, and 2027077 contain the supplementary crystallographic data for this paper. These data can be obtained free of charge via www.ccdc.cam.ac.uk/data_request/cif, or by emailing data_request@ccdc.cam.ac.uk, or by contacting The Cambridge Crystallographic Data Centre, 12 Union Road, Cambridge CB2 1EZ, UK; fax: +44 1223 336033.

AUTHOR INFORMATION

Corresponding Author

Yanchuan Zhao − *Key Laboratory of Organofluorine Chemistry, Center for Excellence in Molecular Synthesis, Shanghai Institute of Organic Chemistry, University of Chinese Academy of Sciences, Chinese Academy of Sciences, Shanghai 200032, China; Key Laboratory of Energy Regulation Materials, Shanghai Institute of Organic Chemistry, Chinese Academy of Sciences, Shanghai 200032, China;* orcid.org/0000-0002-2903-4218; Email: zhaoyanchuan@sioc.ac.cn

Authors

Zhenchuang Xu − *Key Laboratory of Organofluorine Chemistry, Center for Excellence in Molecular Synthesis, Shanghai Institute of Organic Chemistry, University of Chinese Academy of Sciences, Chinese Academy of Sciences, Shanghai 200032, China*

Nie Fang − *Key Laboratory of Organofluorine Chemistry, Center for Excellence in Molecular Synthesis, Shanghai Institute of Organic Chemistry, University of Chinese Academy of Sciences, Chinese Academy of Sciences, Shanghai 200032, China*

Complete contact information is available at: https://pubs.acs.org/10.1021/jacs.0c12223

Notes

The authors declare the following competing financial interest(s): The authors have filed a patent on this technology.

ACKNOWLEDGMENTS

This research was supported by the National Natural Science Foundation of China (21871291, 91956120, 21421002). The authors thank Ms. Xian Cai, Prof. Xin Zhao, and Ms. Shuyan Jiang for their kind help in thermodynamic and kinetic study, and Ms. Lijun Zhang for the ICP-MS test. We also thank Ms. Suzhen Zhu for painting the nepenthes. Y.Z. thanks Fang Wang for the critical reading of the manuscript.

REFERENCES

(1) Lippard, S. J. The Inorganic Side of Chemical Biology. *Nat. Chem. Biol.* **2006**, *2*, 504−507.

(2) Gray, H. B. Biological Inorganic Chemistry at the Beginning of the 21st Century. *Proc. Natl. Acad. Sci. U. S. A.* **2003**, *100*, 3563−3568.

(3) Zoroddu, M. A.; Aaseth, J.; Crisponi, G.; Medici, S.; Peana, M.; Nurchi, V. M. The Essential Metals for Humans: A Brief Overview. *J. Inorg. Biochem.* **2019**, *195*, 120−129.

(4) Gouaux, E.; MacKinnon, R. Principles of Selective Ion Transport in Channels and Pumps. *Science* **2005**, *310*, 1461−1465.

(5) Feske, S.; Skolnik, E. Y.; Prakriya, M. Ion Channels and Transporters in Lymphocyte Function and Immunity. *Nat. Rev. Immunol.* **2012**, *12*, 532−547.

(6) Varma, S.; Sabo, D.; Rempe, S. B. K^+/Na^+ Selectivity in K Channels and Valinomycin: Over-Coordination Versus Cavity-Size Constraints. *J. Mol. Biol.* **2008**, *376*, 13−22.

(7) Pinkerton, M.; Steinrauf, L. K.; Dawkins, P. The Molecular Structure and Some Transport Properties of Valinomycin. *Biochem. Biophys. Res. Commun.* **1969**, *35*, 512−518.

(8) Doyle, D. A. The Structure of the Potassium Channel: Molecular Basis of K^+ Conduction and Selectivity. *Science* **1998**, *280*, 69−77.

(9) Jiang, Y.; Lee, A.; Chen, J.; Cadene, M.; Chait, B. T.; MacKinnon, R. Crystal Structure and Mechanism of a Calcium-Gated Potassium Channel. *Nature* **2002**, *417*, 515−522.

(10) Zhou, Y.; Morais-Cabral, J. H.; Kaufman, A.; Mackinnon, R. Chemistry of Ion Coordination and Hydration Revealed by a K^+ Channel-Fab Complex at 2.0 Å Resolution. *Nature* **2001**, *414*, 43−48.

(11) Kopec, W.; Köpfer, D. A.; Vickery, O. N.; Bondarenko, A. S.; Jansen, T. L. C.; de Groot, B. L.; Zachariae, U. Direct Knock-on of Desolvated Ions Governs Strict Ion Selectivity in K^+ Channels. *Nat. Chem.* **2018**, *10*, 813−820.

(12) Riccardi, L.; Gabrielli, L.; Sun, X.; De Biasi, F.; Rastrelli, F.; Mancin, F.; De Vivo, M. Nanoparticle-Based Receptors Mimic Protein-Ligand Recognition. *Chem.* **2017**, *3*, 92−109.

(13) Hu, X. B.; Chen, Z.; Tang, G.; Hou, J. L.; Li, Z. T. Single-Molecular Artificial Transmembrane Water Channels. *J. Am. Chem. Soc.* **2012**, *134*, 8384−8387.

(14) Xin, P.; Zhu, P.; Su, P.; Hou, J. L.; Li, Z. T. Hydrogen-Bonded Helical Hydrazide Oligomers and Polymer That Mimic the Ion Transport of Gramicidin A. *J. Am. Chem. Soc.* **2014**, *136*, 13078−13081.
(15) Mendez-Arroyo, J.; Barroso-Flores, J.; Lifschitz, A. M.; Sarjeant, A. A.; Stern, C. L.; Mirkin, C. A. A Multi-State, Allosterically-Regulated Molecular Receptor with Switchable Selectivity. *J. Am. Chem. Soc.* **2014**, *136*, 10340−10348.
(16) Shen, J.; Ye, R.; Romanies, A.; Roy, A.; Chen, F.; Ren, C.; Liu, Z.; Zeng, H. Aquafoldmer-Based Aquaporin-like Synthetic Water Channel. *J. Am. Chem. Soc.* **2020**, *142*, 10050−10058.
(17) Huang, W. L.; Wang, X. D.; Ao, Y. F.; Wang, Q. Q.; Wang, D. X. Artificial Chloride-Selective Channel: Shape and Function Mimic of the ClC Channel Selective Pore. *J. Am. Chem. Soc.* **2020**, *142*, 13273−13277.
(18) Li, X.; Zhang, H.; Hou, J.; Ou, R.; Zhu, Y.; Zhao, C.; Qian, T.; Easton, C. D.; Selomulya, C.; Hill, M. R.; Wang, H. Sulfonated Sub-1-Nm Metal-Organic Framework Channels with Ultrahigh Proton Selectivity. *J. Am. Chem. Soc.* **2020**, *142*, 9827−9833.
(19) August, D. P.; Borsley, S.; Cockroft, S. L.; della Sala, F.; Leigh, D. A.; Webb, S. J. Transmembrane Ion Channels Formed by a Star of David [2]Catenane and a Molecular Pentafoil Knot. *J. Am. Chem. Soc.* **2020**, *142*, 18859−18865.
(20) Howe, E. N. W.; Gale, P. A. Fatty Acid Fueled Transmembrane Chloride Transport. *J. Am. Chem. Soc.* **2019**, *141*, 10654−10660.
(21) Acharyya, K.; Bhattacharyya, S.; Sepehrpour, H.; Chakraborty, S.; Lu, S.; Shi, B.; Li, X.; Mukherjee, P. S.; Stang, P. J. Self-Assembled Fluorescent Pt(II) Metallacycles as Artificial Light-Harvesting Systems. *J. Am. Chem. Soc.* **2019**, *141*, 14565−14569.
(22) Izatt, R. M.; Bradshaw, J. S.; Nielsen, S. A.; Lamb, J. D.; Christensen, J. J.; Sen, D. Thermodynamic and Kinetic Data for Cation-Macrocycle Interaction. *Chem. Rev.* **1985**, *85*, 271−339.
(23) Izatt, R. M.; Pawlak, K.; Bradshaw, J. S.; Bruening, R. L. Thermodynamic and Kinetic Data for Macrocycle Interaction with Cations, Anions, and Neutral Molecules. *Chem. Rev.* **1995**, *95*, 2529−2586.
(24) Ghidini, E.; Ugozzoli, F.; Ungaro, R.; Harkema, S.; Abu El-Fadl, A.; Reinhoudt, D. N. Complexation of Alkali Metal Cations by Conformationally Rigid, Stereoisomeric Calix[4]Arene Crown Ethers: A Quantitative Evaluation of Preorganization. *J. Am. Chem. Soc.* **1990**, *112*, 6979−6985.
(25) Casnati, A.; Pochini, A.; Ungaro, R.; Bocchi, C.; Ugozzoli, F.; Egberink, R. J. M.; Struijk, H.; Lugtenberg, R.; De Jong, F.; Reinhoudt, D. N. 1,3-Alternate Calix[4]Arenecrown-5 Conformers: New Synthetic Ionophores with Better K^+/Na^+ Selectivity than Valinomycin. *Chem. - Eur. J.* **1996**, *2*, 436−445.
(26) Prodi, L.; Bolletta, F.; Montalti, M.; Zaccheroni, N.; Casnati, A.; Sansone, F.; Ungaro, R. Photophysics of 1,3-Alternate Calix[4]-Arene-Crowns and of Their Metal Ion Complexes: Evidence for Cation−π Interactions in Solution. *New J. Chem.* **2000**, *24*, 155−158.
(27) Scholl, M.; Ding, S.; Lee, C. W.; Grubbs, R. H. Synthesis and Activity of a New Generation of Ruthenium-Based Olefin Metathesis Catalysts Coordinated with 1,3-Dimesityl-4,5-Dihydroimidazol-2-Ylidene Ligands. *Org. Lett.* **1999**, *1*, 953−956.
(28) Iwema Bakker, W. I.; Haas, M.; Khoo-Beattie, C.; Ostaszewski, R.; Franken, S. M.; den Hertog, H. J.; Verboom, W.; de Zeeuw, D.; Harkema, S.; Reinhoudt, D. N. Kinetically Stable Complexes of Alkali Cations with Calixspherands: An Evaluation of Shielding. *J. Am. Chem. Soc.* **1994**, *116*, 123−133.
(29) Lein, G. M.; Cram, D. J. Host-Guest Complexation. 34. Bridged Hemispherands. *J. Am. Chem. Soc.* **1985**, *107*, 448−455.
(30) Lehn, J. M.; Sauvage, J. P. [2]-Cryptates. Stability and Selectivity of Alkali and Alkaline-Earth Macrobicyclic Complexes. *J. Am. Chem. Soc.* **1975**, *97*, 6700−6707.
(31) Lehn, J.-M. Supramolecular Chemistry: Receptors, Catalysts, and Carriers. *Science* **1985**, *227*, 849−856.
(32) Bock, C. W.; Katz, A. K.; Markham, G. D.; Glusker, J. P. Manganese as a Replacement for Magnesium and Zinc: Functional Comparison of the Divalent Ions. *J. Am. Chem. Soc.* **1999**, *121*, 7360−7372.
(33) Cuello, L. G.; Jogini, V.; Cortes, D. M.; Pan, A. C.; Gagnon, D. G.; Dalmas, O.; Cordero-Morales, J. F.; Chakrapani, S.; Roux, B.; Perozo, E. Structural Basis for the Coupling between Activation and Inactivation Gates in K^+ Channels. *Nature* **2010**, *466*, 272−275.
(34) Cuello, L. G.; Jogini, V.; Cortes, D. M.; Perozo, E. Structural Mechanism of C-Type Inactivation in K^+ Channels. *Nature* **2010**, *466*, 203−208.
(35) Renart, M. L.; Triano, I.; Poveda, J. A.; Encinar, J. A.; Fernández, A. M.; Ferrer-Montiel, A. V.; Gómez, J.; González Ros, J. M. Ion Binding to KcsA: Implications in Ion Selectivity and Channel Gating. *Biochemistry* **2010**, *49*, 9480−9487.

https://dx.doi.org/10.1021/jacs.0c12223
J. Am. Chem. Soc. 2021, 143, 3162−3168